Three-body recombination in heteronuclear mixtures at finite temperature

D. S. Petrov, Felix Werner

Three-body recombination in heteronuclear mixtures at finite temperature

D. S. Petrov[1,*] and F. Werner[2,†]

[1]*Université Paris-Sud, CNRS, LPTMS, UMR8626, F-91405 Orsay, France*

[2]*Laboratoire Kastler Brossel, ENS-PSL, UPMC-Sorbonne Universités, Collège de France, CNRS, 24 rue Lhomond, 75231 Paris Cedex 05, France*

(Received 13 February 2015; published 17 August 2015)

Within the universal zero-range theory, we compute the three-body recombination rate to deep molecular states for two identical bosons resonantly interacting with each other and with a third atom of another species, in the absence of weakly bound dimers. The results allow for a quantitative understanding of loss resonances at finite temperature and, combined with experimental data, can be used for testing the Efimov universality and extracting the corresponding three-body parameters in a given system. Curiously, we find that the loss rate can be dramatically enhanced by the resonant heavy-heavy interaction, even for high mass ratios where this interaction is practically irrelevant for the Efimov scaling factor. This effect is important for analyzing the recent loss measurements in the Cs-Li mixture.

DOI: 10.1103/PhysRevA.92.022704 PACS number(s): 34.50.−s, 03.65.Nk, 67.85.Pq

I. INTRODUCTION

Measuring atomic three-body losses near Feshbach resonances for large and negative scattering lengths has become a major tool for characterizing the Efimov physics in a large variety of ultracold gases, not only for identical bosonic atoms [1–14] but also for homonuclear [15–17] and heteronuclear [18–21] mixtures. The peaks in the three-body loss rate as a function of the magnetic field mark passages of Efimov trimers through the free-atom scattering threshold. If the size of such a trimer is much smaller than the typical de Broglie wavelengths in the gas, the corresponding peak is most visible and is well described by zero-temperature theory [1]. Then, according to the Efimov discrete scaling invariance, the next peak is expected to occur when the two-body scattering length is multiplied by the so-called Efimov period, the trimer being proportionally larger. The Efimov period is numerically quite large, so that when trying to observe multiple successive peaks, i.e., trying to test the Efimov scenario, one very soon faces the problem that Efimov states become too large and the loss rate saturates to a constant value [10,11,14,22].

For identical bosons the Efimov period equals 22.7 [23] and two loss peaks separated by approximately this factor have recently been observed in Cs [12,13]. However, the second (excited-state) peak is already close to the saturation regime and its quantitative characterization has been done relying on the finite-temperature theory developed in Ref. [10] for three identical bosons. Similarly, an Efimov loss feature for large negative scattering lengths in the mixture of three hyperfine states of ^{6}Li has recently been reanalyzed by using a suitable modification of this finite-temperature theory, leading to a better determination of the three-body parameter in this system [17].

The Efimov period is significantly smaller for strongly mass-imbalanced heteronuclear systems [24], making them ideal candidates for testing the Efimov discrete scaling invariance [25]. Very recently, experiments [20,21] have observed more than one period of the Efimov scaling dependence in the system of one Li and two Cs atoms, where the Efimov period is $\simeq$5. For ^{6}Li-^{87}Rb-^{87}Rb this quantity is $\simeq$7 and the Rb-Li mixture is thus also potentially interesting from the viewpoint of testing the Efimov scenario.

In this article we generalize the S-matrix formalism developed for three bosons (case BBB) in Refs. [10] and [26–28] to the case of an atom interacting with two identical bosons (case ABB). We assume that the AB interaction is tuned to the negative side of a Feshbach resonance and consider two cases for the BB interaction: (i) the BB interaction is neglected, and (ii) the BB scattering length is large and negative. Case i is suitable for the Li-Rb-Rb system, while case ii is relevant for the Li-Cs-Cs system in the magnetic field region studied in Refs. [20] and [21]. In neither of these two cases does the system support weakly bound dimers, and therefore, the loss is entirely determined by the recombination to deeply bound states. Under these conditions we express the loss rate constant in terms of the temperature, the three-body parameter, the inelasticity parameter, and a quantity s_{11} which is a function of a single variable, ka_{AB}, in case i and of two variables, ka_{AB} and ka_{BB}, in case ii, where k is the three-body collision momentum. Once this universal function is calculated (and tabulated) for a given AB mass ratio, one can then easily generate loss curves for any given temperature, three-body parameter, and inelasticity parameter.

The article is organized as follows. In Sec. II we introduce basic notations, present a formula for the loss rate constant, and apply it to ^{6}Li-^{87}Rb-^{87}Rb and ^{6}Li-^{133}Cs-^{133}Cs, commenting on the role of the BB interaction. In Sec. III we give a detailed derivation of this loss rate formula. The calculation of the universal function s_{11} is the subject of Sec. IV. Appendixes include the normalization constant and contact parameters for Efimov ABB trimers and the analytic expansion of s_{11} near unitarity, and in Appendix E we show how one can recover the case BBB from the present article.

II. MAIN RESULTS

We start with some reminders about and notations of the three-body problem of two bosons of mass m_B and a third

*petrov@lptms.u-psud.fr
†werner@lkb.ens.fr

particle of mass m_A. We write m for twice the reduced mass,

$$m = 2\frac{m_A m_B}{m_A + m_B}. \quad (1)$$

The mass ratio is conveniently parameterized by the angle

$$\sin\phi = \frac{m_B}{m_A + m_B}. \quad (2)$$

For further convenience we also define

$$\theta = \frac{\pi}{4} - \frac{\phi}{2}. \quad (3)$$

We denote by a_{AB} and a_{BB} the AB and BB scattering lengths.

Universal properties, such as the Efimov discrete scaling invariance, appear in the zero-range limit, which can be described by a universal theory [1,23]. Accordingly, we consider zero-range interactions between A and B particles, while between B particles we assume no interactions in case i and zero-range interactions in case ii. The validity conditions for this universal zero-range theory are the following. In case i, the characteristic interaction ranges and $|a_{BB}|$ should be much smaller than $|a_{AB}|$ and the typical de Broglie wavelengths. In case ii, the characteristic interaction ranges should be much smaller than $|a_{AB}|$, $|a_{BB}|$, and the typical de Broglie wavelengths.

The *unitary limit* is defined by

$$\begin{aligned} a_{AB} &= \infty && \text{in case i,} \\ a_{AB} &= a_{BB} = \infty && \text{in case ii.} \end{aligned} \quad (4)$$

As usual, scattering length values $+\infty$ and $-\infty$ are equivalent. At the unitary limit, the scattering length(s) does(do) not introduce any length scale into the problem. Due to the Efimov effect, there is no continuous scale invariance, but a discrete one. In particular, the energies of Efimov trimers follow a geometric series:

$$E_{n+1}/E_n = e^{-2\pi/s_0}. \quad (5)$$

Here s_0 is the positive real solution of [24]

$$\lambda(s_0,\phi) = 1 \quad \text{in case i,} \quad (6)$$

$$1 - \lambda(s_0,\phi) - 2\lambda^2(s_0,\theta) = 0 \quad \text{in case ii,} \quad (7)$$

where

$$\lambda(s_0,\delta) \equiv \frac{2\sinh(\delta s_0)}{s_0\cosh(\pi s_0/2)\sin(2\delta)}. \quad (8)$$

Note that we do not consider here the case of a very high mass ratio, where additional Efimovian sectors would appear in nonzero total angular momentum subspaces. We thus assume that m_B/m_A is smaller than the critical value $\simeq 40$, where an additional Efimov effect appears in the angular momentum $L = 2$ subspace [24].

The Efimov effect also implies that the interactions within the universal zero-range theory are parameterized not only by the scattering lengths, but also by a three-body parameter. For this purpose we use a length parameter R_0 defined *modulo* multiplication by e^{π/s_0}. This parameter fixes a hyper-radial node of the three-body wave function at small interparticle distances and thus fixes all other three-body observables [see Eq. (C6) for its relation to the spectrum of Efimov trimers].

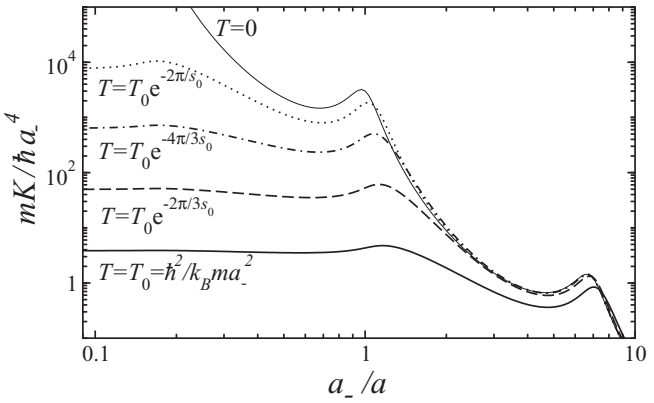

FIG. 1. Event rate constant K (in units of $\hbar a_-^4/m$) versus a_-/a for the ^{6}Li-^{87}Rb-^{87}Rb system for various temperatures with the inelasticity parameter set to $\eta = 0.2$.

To account for recombination losses to deeply bound states in the zero-range theory one allows the three-body parameter to be complex, $R_0 \to R_0\, e^{-i\eta/s_0}$, where $\eta > 0$ is the inelasticity parameter [1]. A precise definition of R_0 and η is given by the three-body contact condition, Eq. (18), below.

Summarizing, the external parameters of the zero-range theory are the scattering length a_{AB}, three-body parameter R_0, and inelasticity parameter η, as well as the scattering length a_{BB} in case ii. Experimentally, all these parameters depend on the magnetic field B. However, essential for universal Efimov physics is only the resonant enhancement of a_{AB} near a Feshbach resonance. In its sufficiently narrow vicinity the other parameters can be assumed constant since their B dependence is smooth. It is important to note that the assumption of constant R_0 and η is not directly related to the applicability conditions of the zero-range approximation mentioned above. In particular, all our derivations and formulas remain valid for B-dependent R_0 and η. However, these parameters are assumed constant in Figs. 1 and 2.

A. Loss rate constant

Our system of interest is a mixture of A and B atoms, in the gaseous nondegenerate regime where the thermal wavelength

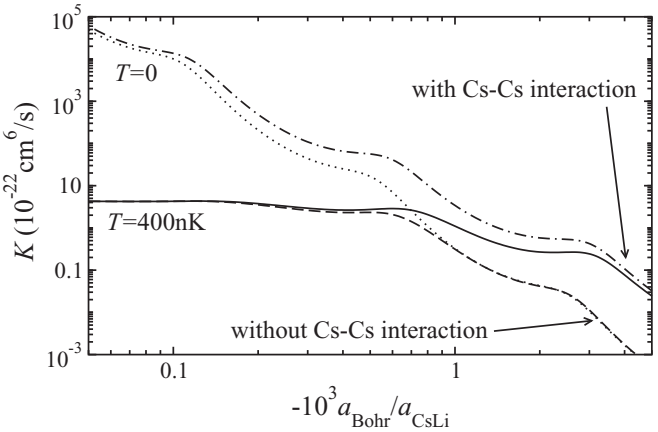

FIG. 2. K vs $-1/a_{CsLi}$ at $T = 0$ and $T = 400$ nK including and excluding the CsCs interaction. Three-body and inelasticity parameters are set to $R_0 = 130 a_{Bohr}$ and $\eta = 0.6$, respectively.

is small compared to the interparticle distances. We do not consider finite positive values of the scattering lengths, where weakly bound dimers would exist; we also assume that a_{AB} is nonzero, in order to have a nontrivial three-body problem.

The rate of ABB recombination events per unit volume is $K\, n_A\, {n_B}^2$, where n_A and n_B are the atom number densities, and K is the event rate constant, for which we obtain

$$K = 64\,\pi^2 \cos^3\phi\ \frac{\hbar^7}{m^4(k_B T)^3}(1 - e^{-4\eta}) \times \int_0^\infty \frac{1 - |s_{11}|^2}{|1 + (kR_0)^{-2is_0} e^{-2\eta}\, s_{11}|^2}\, e^{-\hbar^2 k^2/mk_B T}\, k\, dk. \quad (9)$$

The function s_{11} depends only on ka_{AB}, ka_{BB}, and the mass ratio. Therefore, Eq. (9) gives an explicit dependence of the loss rate on the three-body and inelasticity parameters. This is a manifestation of a general property known as Efimov's radial law [26,27].

For high temperatures or large scattering lengths such that in case i we typically have $-ka_{AB} \gg 1$ and in case ii $-ka_{AB} \gg 1$ and $-ka_{BB} \gg 1$, the function s_{11} in Eq. (9) can be approximated by its asymptotic unitary value,

$$s_{11}^\infty = -e^{-\pi s_0 + i\, 2[s_0 \ln 2 + \arg\Gamma(1 + i s_0)]}, \quad (10)$$

with s_0 given by Eqs. (6,7).

In Sec. IV we show how to compute s_{11} at finite ka_{AB} and ka_{BB} for any given mixture. Once this task is accomplished, Eq. (9) offers a very fast way of calculating the loss rate for any T, R_0, and η and can thus be used for extracting these parameters from experimental data in the universal limit. Obviously, in this manner not only experimental but also theoretical results obtained for finite-range potentials can be compared to the zero-range theory.

In the next two subsections we employ Eq. (9) to calculate K in two experimentally relevant cases characterized by high mass ratios: A = ^{6}Li, B = ^{87}Rb and A = ^{6}Li, B = ^{133}Cs.[1]

B. Lithium-rubidium

We first consider the case A = ^{6}Li, B = ^{87}Rb and neglect the ^{87}Rb-^{87}Rb interaction since it is nonresonant apart from narrow magnetic-field intervals [29,30]. Broad interspecies Feshbach resonances in the hyperfine ground states are available for both ^{6}Li-^{87}Rb and ^{7}Li-^{87}Rb combinations [30–32]. However, for the purpose of testing the Efimov scenario in the ABB system the choice of fermionic A allows one to neglect concomitant AAB losses suppressed due to the fermionic statistics [33].

The ^{6}Li-^{87}Rb-^{87}Rb system is characterized by $s_0 = 1.63188$ and a scaling factor $e^{\pi/s_0} = 6.85610$. In Fig. 1 we present the event rate constant K (in units of $\hbar a_-^4/m$) as a function of a_-/a for different temperatures. Here a is the Rb-Li scattering length and $a_- < 0$ is the position of the three-body loss peak at zero temperature (at $a = a_-$ an Efimov trimer crosses the three-atom threshold). The (three-body) parameter a_- is convenient when there is only one relevant scattering length (for instance, for three identical bosons or for our case i). We find that for the ^{6}Li-^{87}Rb mass ratio a_- is related to R_0 by $a_- \approx -5.233\,R_0$.

The shapes of the curves are controlled by η and T. Unaware of experimental results, we set $\eta = 0.2$. The lowest curve in Fig. 1 corresponds to $T = T_0 = \hbar^2/k_B m a_-^2$ and the other ones are obtained by decreasing $\ln T$ by $2\pi/3s_0$, i.e., a third of the Efimov energetic period. Thus, the solid curve for $T = T_0$ and the dotted one for $T = T_0 e^{-2\pi/s_0}$ are self-similar; the latter can be obtained by shifting the former horizontally by $e^{-\pi/s_0}$ and vertically by $e^{4\pi/s_0}$. The zero-temperature result (thin solid curve) is known analytically [34]. The shift of the resonance peak towards smaller $|a|$ with increasing T is likely to be related to the fact that for $|a| < |a_-|$ the trimer becomes a finite-energy resonance in the three-atom continuum.

C. Lithium-cesium

Because of its higher mass ratio, the combination A = ^{6} Li, B = ^{133} Cs is considered an even better candidate for observing several periods of the Efimov discrete scaling. Two groups have recently reported loss measurements for this mixture close to a wide CsLi Feshbach resonance at 843G [20,21]. The first two Efimov resonances and signatures of the third one have been detected, although the latter is rather strongly thermally saturated.

In treating the ^{6}Li-^{133}Cs-^{133}Cs system for magnetic fields studied in [20] and [21], one must bear in mind that the CsCs scattering length is rather large (about $-1550a_{Bohr}$ at the CsLi resonance [35]) and this may increase the loss rate constant because of the enhanced probability of finding two Cs atoms close to each other. On the other hand, to describe the Efimov effect for such a high mass ratio one is tempted to use the Born-Oppenheimer approximation [36], within which the heavy-heavy interaction is irrelevant for the discrete scaling. Indeed, the ^{6}Li-^{133}Cs-^{133}Cs system in case i is characterized by a scaling factor $e^{\pi/s_0} = 4.87661$ [Eq. (6) gives $s_0 = 1.98277$], whereas for $a_{CsCs} = \infty$ this quantity becomes 4.79887 [$s_0 = 2.00308$ as follows from Eq. (7)] (cf. [37]).

In Fig. 2 we plot K vs $-1/a_{CsLi}$ for $T = 400$ nK (solid and dashed curves) and $T = 0$ (dash-dotted and dotted curves), with $R_0 = 130a_{Bohr}$ and $\eta = 0.6$. Including the CsCs interaction we obtain the solid and dash-dotted curves, whereas neglecting it gives the dashed and dotted lines. In the CsCs-interacting case we use the magnetic-field dependence $a_{CsCs}(B)$ provided in the Suplemental Material to Ref. [35] and eliminate the magnetic field by using the formula $a_{CsLi} = -28.5a_{Bohr}[61.4G/(B - 842.9G) + 1]$ [20]. A different $a_{CsLi}(B)$ was used in Ref. [21], and Ref. [38] gives yet another more recent characterization of $a_{CsLi}(B)$. For the results plotted in Fig. 2 these variations are not very important because $a_{CsCs}(B)$ is smooth, and therefore, the dependence $a_{CsCs}(a_{CsLi})$ is practically unchanged.

Figure 2 clearly shows that the effect of finite T is to saturate K at large a_{CsLi}, whereas the inclusion of the CsCs interaction leads to a strong enhancement of the loss rate for small a_{CsLi}. For the experimentally studied region of B either of these effects can lead to corrections of two orders of magnitude. The overall behavior of K is thus much less steep than the scaling $K \propto a_{CsLi}^4$ (compare solid and dotted lines in Fig. 2),

[1]Tabulated values of s_{11} for these systems can be obtained by contacting the authors.

consistent with the experimental findings [20,21]. The peak positions move when we "switch on" the CsCs interaction, but this is an artifact of choosing the same R_0 in these two cases. In fact, even in the limit $a_{\rm CsLi} \to \infty$ the loss features are not expected to exactly match. This is because the Efimovian type ii wave function has to propagate through distances of order $a_{\rm CsCs}$ before it can be matched with the type i wave function. In general, when both case i and case ii are applicable, i.e., when $|a_{\rm BB}|$ is much larger than the characteristic interaction ranges but smaller than $|a_{\rm AB}|$ and $1/k$, the corresponding three-body parameters are related to each other by the wave-function matching condition but are not necessarily equal.

The parameters $R_0 = 130 a_{\rm Bohr}$ and $\eta = 0.6$ used to plot Fig. 2 have been chosen as a result of a very approximate fitting of the data in Refs. [20] and [21]. A significantly more serious account of experimental uncertainties and cross-correlations is needed to give a more definite answer for R_0 and η. We find that the fitting procedure is very sensitive to the exact position of the Feshbach resonance. Surely, one would benefit from more experimental data at lower temperatures. Setting $T = 0$, $\eta \ll 1$, and $R_0 = 130 a_{\rm Bohr}$ we obtain sharp peaks of K at positions $a_{\rm CsLi} = a_-^{(0)} \approx -330 a_{\rm Bohr}$, $a_{\rm CsLi} = a_-^{(1)} \approx -1.7 \times 10^3 a_{\rm Bohr}$, and $a_{\rm CsLi} = a_-^{(2)} \approx -8.8 \times 10^3 a_{\rm Bohr}$, which compares very well with the refined analysis of the experimental data performed in Ref. [38].

We note that the experiments in [20] and [21] are well within the zero-range limit, at least, for the second and higher Efimov resonances. Indeed, of the van der Waals ranges [30,39], the Feshbach resonance parameters R_* [30,40,41], and the length $\sqrt{R_*|a_{\rm bg}|}$ that enters when the background scattering length $a_{\rm bg}$ is negative [42], the largest is the Cs-Cs van der Waals range $r_{\rm vdW,CsCs} = 101 a_{\rm Bohr}$. In turn, this quantity is much smaller than the thermal wavelengths ($>3400\, a_{\rm Bohr}$ at $T < 800$ nK) and the Cs-Cs scattering length, which, for experimentally relevant magnetic fields, varies in the interval $-1550 a_{\rm Bohr} < a_{\rm CsCs} < -900 a_{\rm Bohr}$ [35]. As far as the Cs-Li scattering length is concerned, around the first Efimov resonance it approximately equals $-300 a_{\rm Bohr}$, which is comparable to $r_{\rm vdW,CsCs}$. However, for the second and higher resonances the inequality $|a_{\rm CsLi}| \gg r_{\rm vdW,CsCs}$ is well satisfied.

Wang *et al.* [43] have studied the so-called van der Waals universality of the three-body parameter in heteronuclear systems close to a wide interspecies resonance by assuming the Lennard-Jones interatomic potentials. According to their analytical estimates in the case of a large mass imbalance the three-body parameter equals the heavy-heavy van der Waals range $r_{\rm vdW,BB}$ times a dimensionless function of the ratio $r_{\rm vdW,BB}/a_{\rm BB}$. For the Cs-Cs-Li case in the experimentally relevant region this function varies very little ($<2\%$) since the ratio $r_{\rm vdW,CsCs}/a_{\rm CsCs}$ stays low. We mention for reference that for $a_{\rm CsCs} = 2000 a_{\rm Bohr}$ Ref. [43] predicts $a_- = -1.4 \times 10^3 a_{\rm Bohr}$.

A finite-temperature theoretical analysis of losses in this system has been performed by Y. Wang and reported in the Supplemental Material to Ref. [21]. Wang's results indicate that with increasing temperature the resonance features become weaker and shift towards smaller $a_{\rm CsLi}$, which is what we also observe. In fact, we can rather well fit Wang's curves for all three considered temperatures ($T = 100$ nK, 250 nK, and 1 μK) by choosing $R_0 = 110 a_{\rm Bohr}$ and $\eta = 0.4$.

III. DERIVATION OF THE LOSS RATE CONSTANT

In this section, we derive the expression, (9), for the loss rate constant in terms of the quantity s_{11}, as well as the analytical result, (10), for s_{11} valid at the unitary limit.

Let us first introduce the three-body scattering state ψ. Denoting the positions of the two identical bosons $\mathbf{r}_1$ and $\mathbf{r}_3$, and the position of the third particle $\mathbf{r}_2$, the wave function $\psi(\mathbf{r}_1,\mathbf{r}_2,\mathbf{r}_3)$ is symmetric with respect to exchanging $\mathbf{r}_1$ and $\mathbf{r}_3$.

Let us introduce the Jacobi coordinates

$$\cos\phi\ \mathbf{x} = \mathbf{r}_3 - \frac{m_{\rm A}\mathbf{r}_2 + m_{\rm B}\mathbf{r}_1}{m_{\rm A} + m_{\rm B}}, \quad \mathbf{y} = \mathbf{r}_2 - \mathbf{r}_1. \tag{11}$$

All information about the relative positions of the three particles can then be collected in the six-dimensional vector

$$\mathbf{R} = (\mathbf{x},\mathbf{y}). \tag{12}$$

Its norm $R = \sqrt{x^2 + y^2}$ is the so-called hyper-radius, while its direction

$$\mathbf{\Omega} \equiv \mathbf{R}/R$$

can be parameterized by five hyperangles. One can note that if all particle coordinates are multiplied by a factor λ, then the hyper-radius is multiplied by λ while the hyperangles are unchanged.

At large distances, the scattering-state asymptotes to an incoming plane wave plus a scattered wave. More precisely, in the center-of-mass reference frame,

$$\psi(\mathbf{R}) \underset{R\to\infty}{\simeq} \psi^{(0)}(\mathbf{R}) + \psi_{\rm sc}(\mathbf{R}), \tag{13}$$

where $\psi_{\rm sc}(\mathbf{R})$ is a purely outgoing scattered wave, and

$$\psi^{(0)}(\mathbf{R}) = \frac{1+P}{\sqrt{2}}\, e^{i\mathbf{k}\cdot\mathbf{R}} \tag{14}$$

is a symmetrized plane wave, normalized in a unit volume. The operator P in Eq. (14) exchanges particles 1 and 3. The relation between k and the collision energy is

$$E = \frac{k^2}{m}. \tag{15}$$

Here and in what follows, we set $\hbar = 1$.

Furthermore, ψ is an eigenstate of the zero-range model; i.e., it satisfies

(a) the Schrödinger equation

$$-\frac{1}{m}\Delta_{\mathbf{R}}\psi(\mathbf{R}) = E\,\psi(\mathbf{R}) \tag{16}$$

when none of the three particle positions coincide;

(b) the two-body contact conditions: for each interacting pair of particles i,j, $\exists A_{ij}$ such that

$$\psi \underset{r_{ij}\to 0}{=} \left(\frac{1}{r_{ij}} - \frac{1}{a_{ij}}\right) A_{ij} + o(1), \tag{17}$$

where A_{ij} depends on the relative position of the third particle with respect to the center of mass of particles i and j; and

(c) the three-body contact condition: $\exists B$ such that

$$\psi(\mathbf{R}) \underset{R\to 0}{\sim} \left[\left(\frac{R}{R_0}\right)^{-is_0} - e^{-2\eta}\left(\frac{R}{R_0}\right)^{is_0}\right] \frac{B(\mathbf{\Omega})}{R^2}. \tag{18}$$

The loss rate can then be obtained from the scattering state thanks to the following exact relation, which can be justified by heuristic arguments. Introducing the probability current

$$\mathbf{J} = \frac{2}{m}\,\mathrm{Im}(\psi^*\,\boldsymbol{\nabla}_{\mathbf{R}}\psi) \tag{19}$$

and the lost flux

$$\varphi_{\mathrm{loss}} = -\oint_{\mathcal{S}} \mathbf{J}\cdot\mathbf{d^5S}, \tag{20}$$

where $\mathcal{S}$ is a hypersurface enclosing the origin (e.g., a hypersphere) and the surface-element vector $\mathbf{d^5S}$ points away from the origin, the loss rate constant is given by the thermal average

$$K = \frac{\int K(k)\,e^{-k^2/mk_BT}\,d^6k}{\int e^{-k^2/mk_BT}\,d^6k} \tag{21}$$

of the energy-resolved event rate constant

$$K(k) = \frac{\cos^3\phi}{2}\,\langle\varphi_{\mathrm{loss}}\rangle_{\hat{k}}, \tag{22}$$

where $\langle.\rangle_{\hat{k}}$ denotes the average over the direction of $\mathbf{k}$. In Eq. (22), the factor $1/2$ originates from the indistinguishability of the two B particles, and the factor $\cos^3\phi$ from the Jacobian of the change of variables from Cartesian to Jacobi coordinates,

$$\left|\frac{\partial(\mathbf{r}_1,\mathbf{r}_2,\mathbf{r}_3)}{\partial(\mathbf{C},\mathbf{x},\mathbf{y})}\right| = \cos^3\phi, \tag{23}$$

where $\mathbf{C}$ is the center of mass of the three particles.

A. Unitary limit

Let us first consider the unitary limit, Eq. (4), where the situation is particularly clear, because the problem can be solved in a fully analytical way. The key ingredient is that there is a separability between the hyper-radius R and the hyperangles $\boldsymbol{\Omega}$, because the two-body contact conditions, (17), do not introduce any length scale and hence act only on the hyperangles [24]. The solutions of the hyperangular part of the three-body problem are the functions $\phi_s(\boldsymbol{\Omega})$ that satisfy the two-body contact condition and which are eigenfunctions of the Laplacian operator on the hypersphere:

$$T_{\boldsymbol{\Omega}}\,\phi_s(\boldsymbol{\Omega}) = -s^2\phi_s(\boldsymbol{\Omega}). \tag{24}$$

The operator $T_{\boldsymbol{\Omega}}$ is defined as the hyperangular part of the total Laplacian

$$\Delta_{\mathbf{R}} = \frac{1}{R^2}\left(\frac{\partial^2}{\partial R^2} + \frac{1}{R}\frac{\partial}{\partial R} + \frac{1}{R^2}T_{\boldsymbol{\Omega}}\right)R^2. \tag{25}$$

We can then expand the scattering state as

$$\psi(\mathbf{R}) = \sum_s \frac{F_s(R)}{R^2}\,\phi_s(\boldsymbol{\Omega}). \tag{26}$$

Indeed, the functions ϕ_s, normalized to unity, form an orthogonal basis for the hyperangular scalar product

$$(f|g) \equiv \int f(\boldsymbol{\Omega})^*\,g(\boldsymbol{\Omega})\,d\boldsymbol{\Omega} \tag{27}$$

(where $d\boldsymbol{\Omega}$ stands for the differential solid angle in six-dimensional space, i.e., $d^6R = d\boldsymbol{\Omega}\,R^5\,dR$). This follows from the self-adjointness of the zero-range model.

In the present case, where the B particles are bosonic and the mass ratio is not very high, the set $\{s\}$ contains a single imaginary value $s = is_0$, where s_0 solves Eq. (6), and an infinite countable set of real values. The $s = is_0$ sector is called Efimovian, since it causes the Efimov effect.

The hyper-radial Schrödinger equation reads

$$\left(-\frac{d^2}{dR^2} - \frac{1}{R}\frac{d}{dR} + \frac{s^2}{R^2}\right)F_s(R) = mE\,F_s(R); \tag{28}$$

i.e., the unitary three-body problem reduces to a set of independent one-body problems in effective s^2/R^2 potentials. The hyper-radial wave functions $F_s(R)$ have the large-distance behavior

$$F_s(R) \underset{R\to\infty}{\simeq} [A^{\mathrm{in}}(s)\,e^{-ikR} + A^{\mathrm{out}}(s)\,e^{ikR}]\sqrt{\frac{m}{2kR}}, \tag{29}$$

where a normalization to unit flux is introduced for later convenience. For the real values of s, due to the repulsive effective potential s^2/R^2, the wave function $F_s(R)$ vanishes for $R\to 0$ (in the absence of three-body resonance), and $|A^{\mathrm{in}}(s)| = |A^{\mathrm{out}}(s)|$; i.e., the scattering is purely elastic. The losses thus come exclusively from the Efimovian sector. There, the strongly attractive effective potential $-s_0^2/R^2$ gives rise to logarithmic waves at small hyper-radii (i.e., in the limit where all three particles are close),

$$F_{is_0}(R) \underset{R\to 0}{\simeq} \left[A_1^{\mathrm{in}}\,e^{is_0\ln(kR)} + A_1^{\mathrm{out}}\,e^{-is_0\ln(kR)}\right]\sqrt{\frac{m}{2s_0}}, \tag{30}$$

where a unit-flux normalization is again introduced for later convenience. The three-body contact condition, Eq. (18), becomes

$$A_1^{\mathrm{in}} = \mathcal{A}\,A_1^{\mathrm{out}}, \tag{31}$$

where

$$\mathcal{A} \equiv -(kR_0)^{-i2s_0}\,e^{-2\eta} \tag{32}$$

has the meaning of a reflection amplitude from the point $R = 0$ (where all particle positions coincide). While the phase of this reflection amplitude is determined by the three-body parameter R_0, its modulus is determined by the inelasticity parameter η, the reflection probability being $|\mathcal{A}|^2 = e^{-4\eta}$. Accordingly,

$$\varphi_{\mathrm{loss}} = (1 - e^{-4\eta})\left|A_1^{\mathrm{out}}\right|^2 \tag{33}$$

[as obtained by taking a vanishingly small hypersphere for $\mathcal{S}$ in Eq. (20)].

In what follows we denote by $A_3^{\mathrm{in/out}}$ the long-distance amplitudes $A^{\mathrm{in/out}}(is_0)$ [see Eq. (29)].[2] The out-amplitudes can be expressed in terms of the in-amplitudes through a linear relation,

$$\begin{pmatrix} A_1^{\mathrm{out}} \\ A_3^{\mathrm{out}} \end{pmatrix} = \begin{pmatrix} s_{11} & s_{13} \\ s_{31} & s_{33} \end{pmatrix}\begin{pmatrix} A_1^{\mathrm{in}} \\ A_3^{\mathrm{in}} \end{pmatrix}. \tag{34}$$

[2]The subscript 3 is used here since the subscript 2 is traditionally reserved for the atom weakly-bound-dimer channel [26–28].

Combining this with Eq. (31) yields

$$A_1^{\rm out} = \frac{s_{13}}{1 - s_{11}\mathcal{A}}\, A_3^{\rm in}. \tag{35}$$

The S matrix s_{ij} is easily computed by using the fact that $F_{is_0}(R)$ is a linear combination of the Bessel functions $J_{\pm is_0}(kR)$. This yields the expression of s_{11} given in Eq. (10). Furthermore, the obtained matrix is unitary, so that $|s_{13}|^2 = 1 - |s_{11}|^2$ and thus

$$\varphi_{\rm loss} = \mathcal{P}\left|A_3^{\rm in}\right|^2, \tag{36}$$

where the recombination loss probability $\mathcal{P}$ equals (compare with Ref. [44])

$$\mathcal{P} = (1 - e^{-4\eta})\,\frac{1 - |s_{11}|^2}{|1 - s_{11}\mathcal{A}|^2}. \tag{37}$$

The last ingredient is that the large-distance in-amplitude $A_3^{\rm in}$ is determined by the projection of the incoming plane wave onto the Efimovian sector. More precisely, the hyperangular overlap $(\phi_{is_0}|\psi^{(0)}) = \sqrt{2}\int d^5\mathbf{\Omega}\,\phi_{is_0}(\mathbf{\Omega})\,e^{i\mathbf{k}\cdot\mathbf{R}}$ can be evaluated for $R \to \infty$ using the stationary-phase method, with a result of the form

$$\left[A_3^{\rm in\,(0)}\,e^{-ikR} + A_3^{\rm out\,(0)}\,e^{ikR}\right]\sqrt{\frac{m}{2k}}\,R^{-5/2}; \tag{38}$$

then $A_3^{\rm in} - A_3^{\rm in\,(0)}$ must vanish, because $(\phi_s|\psi - \psi^{(0)})$ has to behave like a purely outgoing wave at $R \to \infty$, by definition of the scattering state ψ [cf. Eq. (13)]. This yields

$$A_3^{\rm in} = 2^{7/2}\,\pi^{5/2}\,e^{i\,5\pi/4}\,m^{-1/2}\,k^{-2}\,\phi_{is_0}(-\hat{k})^*. \tag{39}$$

Inserting this into Eqs. (36) and (22), ϕ_s drops out after the hyperangular average:

$$K(k) = \frac{64\,\pi^2\,\cos^3\phi}{mk^4}\,(1 - e^{-4\eta})\,\frac{1 - |s_{11}|^2}{|1 - s_{11}\mathcal{A}|^2}. \tag{40}$$

The final expression, Eq. (9), follows immediately.

B. Finite scattering lengths

We turn to the general case where the scattering length(s) is(are) not restricted to the unitary limit, Eq. (4). We will see that the final expression for the loss rate, Eq. (9), remains valid, provided the definition of s_{11} is appropriately generalized. Since the scale invariance of the two-body contact conditions is broken, the separability in hyperspherical coordinates no longer holds. Instead, we follow an S-matrix approach.

We consider the state Ψ_1 that physically corresponds to a stationary triatomic flow injected at the origin of the six-dimensional space (i.e., at $\mathbf{R} = \mathbf{0}$) that gets partially reflected back and partially transmitted towards infinity. More precisely, Ψ_1 is defined as the solution of the Schrödinger equation, (16), with energy $E = k^2/m$ satisfying the two-body contact condition, (17), and having the asymptotes

$$\Psi_1(\mathbf{R}) \underset{R\to 0}{\simeq} \frac{(kR)^{is_0} + s_{11}(kR)^{-is_0}}{R^2}\sqrt{\frac{m}{2s_0}}\,\phi_{is_0}(\mathbf{\Omega}) \tag{41}$$

and

$$\Psi_1(\mathbf{R}) \underset{R\to\infty}{\simeq} s_{31}\,e^{ikR}\sqrt{\frac{m}{2kR}}\,\frac{1}{R^2}\,\Phi_3(\mathbf{\Omega}). \tag{42}$$

Together with the normalization $(\Phi_3|\Phi_3) = 1$, this defines the reflection and transmission amplitudes s_{11} and s_{31}, as well as the function $\Phi_3(\mathbf{\Omega})$ (up to multiplication of s_{31} and Φ_3 by arbitrary phase factors $e^{i\gamma}$ and $e^{-i\gamma}$, respectively). Equation (41) is applicable in the *scale-invariant region*, which we can define by $R \ll \min(|a_{\rm AB}|, 1/k)$ in case i and $R \ll \min(|a_{\rm AB}|, |a_{\rm BB}|, 1/k)$ in case ii. Equation (42) is applicable in the *asymptotic region*, $R \gg \min(|a_{\rm AB}|, 1/k)$ in case i and $R \gg \min[\max(|a_{\rm AB}|, |a_{\rm BB}|), 1/k]$ in case ii.

Then let $\{\Phi_n(\mathbf{\Omega})\}_{n\geqslant 4}$ be an arbitrary orthonormal set of functions such that $\{\Phi_n(\mathbf{\Omega})\}_{n\geqslant 3}$ forms an orthonormal basis [for the scalar product $(.|.)$ defined in Eq. (27)]. A complete set of incoming and outgoing asymptotic states can be defined as

$$\psi_1^{\rm in} \equiv e^{is_0\ln(kR)}\sqrt{\frac{m}{2s_0}}\,\frac{1}{R^2}\,\phi_{is_0}(\mathbf{\Omega}), \tag{43}$$

$$\psi_n^{\rm in} \equiv e^{-ikR}\sqrt{\frac{m}{2kR}}\,\frac{1}{R^2}\,\Phi_n(\mathbf{\Omega})^*, \quad n \geqslant 3, \tag{44}$$

and $\psi_n^{\rm out} \equiv (\psi_n^{\rm in})^*$ for any n in the set $\mathcal{C} \equiv \{1\} \cup \{n;\ n \geqslant 3\}$. The terms incoming and outgoing are meant with respect to the *intermediate region* contained between the scale-invariant and the asymptotic regions.

For an arbitrary solution Ψ of Eqs. (16) and (17), the in- and out-amplitudes $A_n^{\rm in/out}$ can be defined by

$$\Psi \underset{R\to 0}{\simeq} A_1^{\rm in}\,\psi_1^{\rm in} + A_1^{\rm out}\,\psi_1^{\rm out}, \tag{45}$$

$$\Psi \underset{R\to\infty}{\simeq} \sum_{n\geqslant 3}\left[A_n^{\rm in}\,\psi_n^{\rm in} + A_n^{\rm out}\,\psi_n^{\rm out}\right]. \tag{46}$$

The out- and in-amplitudes are linearly related:

$$A_n^{\rm out} = \sum_{m\in\mathcal{C}} s_{nm}\,A_m^{\rm in}, \tag{47}$$

where the matrix s_{nm} is unitary and symmetric, as shown in Appendix A. Furthermore, s_{nm} is independent of the three-body and inelasticity parameters R_0 and η, and depends only on $ka_{\rm AB}$, $ka_{\rm BB}$, and the mass ratio; indeed, we did not impose that Ψ satisfy Eq. (18) as the three-body boundary condition.

This problem of an *a priori* infinite number of coupled channels actually reduces to only two channels. Indeed, channels 1 and 3 decouple from the others; i.e., Eq. (34) remains valid. To check this, first note that $s_{n1} = 0$ for $n \geqslant 4$ by construction [cf. Eq. (42)]. Furthermore, s_{n3} also vanishes for $n \geqslant 4$, because the state with a purely incoming wave in channel 3 (denoted Ψ_3 in Appendix A) is a linear combination of Ψ_1 and Ψ_1^*.

The rest of the reasoning closely follows the $a = \infty$ case. Equations (31)–(33) hold, and hence also Eq. (35). The s matrix being unitary, Eq. (36) follows. It remains to relate $A_3^{\rm in}$ to the projection of the incoming plane wave onto channel 3. For $R \to \infty$, the overlap $(\Phi_3^*|\psi^{(0)})$ can again be evaluated using the stationary-phase method, with a result of the form Eq. (38). On the other hand, the overlap $(\Phi_3^*|\psi)$ behaves at large R as $A_3^{\rm in}\,e^{-ikR}\sqrt{m/(2kR)}\,R^{-2}$ plus an outgoing wave. Since $(\Phi_3^*|\psi - \psi^{(0)})$ still has a purely outgoing behavior at large R, $A_3^{\rm in} - A_3^{\rm in\,(0)} = 0$, which finally gives Eq. (39) with $\phi_{is_0}^*$ replaced by Φ_3. After hyperangular averaging, Φ_3 drops

out of the final expressions, Eqs. (40) and (9). This happens because we consider a nondegenerate gas at equilibrium, whose momentum distribution follows the Boltzman law, so that the three-body momentum distribution depends only on the center-of-mass momentum and on k, and not on $\hat{k}$; in general the functional form of $\Phi_3(\mathbf{\Omega})$ does play a role (see, for example, the study of nonequilibrium effects in Ref. [45]).

C. Analogy with an interferometer

It has been noted [27,28] that the loss peaks can be explained by multiple reflections of the hyper-radial wave off the intermediate region leading to a resonant denominator under the integral in Eq. (9). This behavior becomes transparent if we observe that the considered three-body inelastic scattering problem is formally analogous to a simple interferometer with two partially reflecting mirrors (see Fig. 3). The first mirror (located at intermediate R) has reflection and transmission amplitudes given by the 2×2 matrix

$$\begin{pmatrix} s_{11} & s_{13} \\ s_{31} & s_{33} \end{pmatrix}.$$

The second mirror (located at $R = 0$ within the zero-range model) has the reflection amplitude $\mathcal{A}$, which depends on the three-body parameter and the inelasticity parameter [cf. Eq. (32)]; transmission through this mirror corresponds to the three-body loss process and happens with probability $1 - e^{-4\eta}$.

It then becomes clear that the loss probability is modulated by the interference between the different pathways corresponding to multiple reflections by the two mirrors. More precisely, rewriting the term $1/(1 - s_{11}\mathcal{A})$ in Eq. (35) as $\sum_{n\geqslant 0}(s_{11}\mathcal{A})^n$, the nth-order term corresponds to the pathway with n reflections by each mirror. This is the origin of the term $|1 + (kR_0)^{-2is_0}e^{-2\eta}\, s_{11}|^{-2} = |1/(1 - s_{11}\mathcal{A})|^2$ in the final expression, Eq. (9). This also clarifies why the dependence of the loss rate on R_0 and η is known analytically, s_{11} being independent of these parameters.

The interferometer analogy also physically explains why the energy-dependent event rate constant $K(k)$ has the upper bound

$$K(k) \leqslant K_{\max}(k) = \frac{64\,\pi^2\,\cos^3\phi}{mk^4}. \tag{48}$$

This bound is a manifestation of the fact that the loss happens through a single Efimovian channel at short distance (channel 1), which is coupled to a single large-distance channel (channel 3). The bound is reached when a perfect destructive interference leads to $A_3^{\text{out}} = 0$. The lost flux φ_{loss} is then equal to the incoming flux from infinity $|A_3^{\text{in}}|^2$ (which is determined by a projection of the incoming plane wave, as we have seen). After thermal averaging, Eq. (48) implies

$$K < K_{\max} = \frac{32\,\pi^2\,\cos^3\phi\,\hbar^5}{m^3(k_B T)^2}, \tag{49}$$

where the inequality is now strict since $K(k) = K_{\max}(k)$ cannot hold for all k (and we restored the $\hbar$ dependence).

As a side remark we note that in the case where the B particles are fermionic, with $m_{\text{B}}/m_{\text{A}} \in (13.606\,96\ldots; 75.994\,49\ldots)$ so that the Efimov effect occurs in the total angular momentum $L = 1$ subspace but not in higher L subspaces [24,46,47], the bounds, Eqs. (48) and (49), are multiplied by 3, due to the three Efimovian sectors with angular momentum projections $M = -1$, 0, and $+1$.

Let us now briefly address the low-energy limit. When $ka \to 0^-$ we have $|s_{11}| \to 1$, i.e., the first mirror becomes nearly perfectly reflecting. If η is small enough, the second mirror is also of good quality, and the finesse of the interferometer becomes sufficiently high to observe resonances in the variation of the loss rate with scattering length. The resonances occur when a is such that there exists an Efimov trimer of vanishing energy. This happens when $s_{11}\mathcal{A} \approx 1$, i.e., when the interfering pathways nearly lead to a divergence of $(1 - s_{11}\mathcal{A})^{-1}$ [26]. This naturally leads to peaks in the loss rate constant K versus magnetic field, which remain visible and approximately unshifted after thermal averaging at low enough temperature.

Finally, let us discuss the temperature dependence of the loss rate at the unitary limit in case i (see also [44]). From Eqs. (9) and (10), one finds a qualitatively different behavior depending on the order of magnitude of $|s_{11}^{\infty}| = e^{-\pi s_0}$. When the mass ratio m_B/m_A is sufficiently high, as in the Li-Rb mixture discussed above, $e^{-\pi s_0}$ is small compared to unity, so that s_{11}^{∞} can be neglected to a good approximation in Eq. (9), leading to $K \approx (1 - e^{-4\eta})K_{\max} \propto 1/T^2$. In the language of the interferometer, this means that the first mirror is almost transparent, so that interference effects are negligible. The situation changes when m_B/m_A is not large, e.g., for the mixtures ^{6}Li-^{7}Li, ^{85}Rb-^{87}Rb, or ^{40}K-^{87}Rb (for which nonoverlapping Feshbach resonances are indeed available [30]). Then there is significant reflection from the first mirror, and interference effects lead to noticeable log-periodic oscillations of $K\,T^2$ as a function of T. To observe an entire period of these oscillations experimentally is challenging, since this would require changing T by the large factor $e^{2\pi/s_0}$. However, some T dependence of $K\,T^2$ may be detectable.

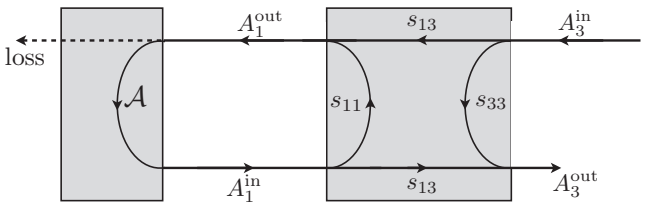

FIG. 3. A three-body wave arriving from large hyper-radii R with amplitude A_3^{in} in the triatomic channel can follow various pathways before it either returns to large R or gets lost at $R = 0$ by turning into an atom and a deep dimer. There is a formal analogy with a Fabry-Perot interferometer with two partially reflecting mirrors.

D. Relation to previous work

Let us comment on the similarities and differences between the approach presented here (and introduced in Ref. [10] in the BBB case) and previous work on three-boson scattering within the zero-range theory [26–28]. Formally, it is possible to derive Eq. (9) starting from the S-matrix formalism in Refs. [26–28]. However, the present approach is physically more transparent. A key point is that we directly constructed the relevant

large-distance triatomic channel and its hyperangular wave function $\Phi_3(\mathbf{\Omega})$ [cf. Eqs. (41) and (42)]. To this end, we considered the wave function Ψ_1, corresponding to a triatomic flow injected at the origin. The idea of this wave function Ψ_1 was already present in Ref. [26], where Efimov introduced the concept of an s matrix connecting short-distance with long-distance hyper-radial motion. However, Ref. [26] focused mainly on the case of negative total energy, where the only open channel at large distances corresponds to the motion of an atom relative to a weakly bound dimer, while triatomic motion is energetically forbidden. Braaten and Hammer [27] added a triatomic large-distance channel charaterized by a wave function independent of the hyperangles. The resulting s matrix provides a suitable framework for studying three-body recombination in a Bose gas with finite a in the zero-temperature limit. Then, in Ref. [28] this formalism was generalized to finite temperatures by using a complete set of long-distance channels with hyperangular wave functions defined by hyperspherical harmonics. A conceptual difficulty with this construction is that these large-distance channels only decouple for $R \gg |a|$, so that one has to formally work with a finite a. In contrast, one would expect physically a smooth dependence on $1/a$ in the interval $(-\infty; 0]$. This expectation is confirmed by the present construction. The shape of the function $\Phi_3(\mathbf{\Omega})$ depends only on ka and interpolates between two limits: for small $k|a|$ it is a constant independent of $\mathbf{\Omega}$ and for large $k|a|$ it tends to $\phi_{is_0}(\mathbf{\Omega})$, the asymptotic region in this case being defined by $R \gg 1/k$. Incidentally, this illustrates the breakdown of the adiabatic hyperspherical approximation for $k|a| \sim 1$.

IV. CALCULATION OF THE FUNCTION s_{11}

Our computational method for the universal function $s_{11}(ka_{\rm AB}, ka_{\rm BB})$ consists of finding the three-body wave function Ψ_1 defined by Eqs. (41) and (42) numerically. We consider case ii, while case i is treated similarly *modulo* the simplifications listed at the end of this section. Analytic results for s_{11} near the unitary limit are presented in Appendix D.

The Schrödinger equation together with the two-body contact condition for the wave function $\Psi_1(\mathbf{R})$ can be reduced to a set of coupled integral Skorniakov and Ter-Martirosian (STM) equations for the functions $f_{\rm AB}$ and $f_{\rm BB}$ defined by

$$f_{\rm AB}(\mathbf{x}) = 4\pi \lim_{y\to 0} y\,\Psi_1, \quad f_{\rm BB}(\mathbf{X}) = 4\pi \lim_{Y\to 0} Y\,\Psi_1, \quad (50)$$

where $(\mathbf{x},\mathbf{y})$ are the Jacobi coordinates given in Eqs. (11), while $(\mathbf{X},\mathbf{Y})$ is another set of Jacobi coordinates defined by

$$\cos\theta\ \mathbf{X} = \mathbf{r}_2 - (\mathbf{r}_1+\mathbf{r}_3)/2, \quad 2\sin\theta\ \mathbf{Y} = \mathbf{r}_3 - \mathbf{r}_1. \quad (51)$$

The STM equations conserve the angular momentum and, in the considered regime where the mass ratio is not very high, the Efimovian solution appears only in the channel with zero angular momentum, so that $f_{ij}(\mathbf{x}) = f_{ij}(x)$. For this reason the contribution of higher angular momentum channels to the loss vanishes in the zero-range limit, in contrast to the three-body recombination into a weakly bound state for positive a when ka is not small [28]. For more details on the derivation of the STM equations in the general case of different masses and scattering lengths, see, for example, Ref. [40]. The asymptotic behavior of Ψ_1 at small hyper-radii given in Eq. (41) translates into

$$\begin{bmatrix} f_{\rm AB}(x) \\ f_{\rm BB}(x) \end{bmatrix} \underset{x\to 0}{\simeq} \begin{pmatrix} C_{\rm AB} \\ C_{\rm BB} \end{pmatrix} \frac{(kx)^{is_0} + s_{11}(kx)^{-is_0}}{x}, \quad (52)$$

where $C_{\rm AB}$ and $C_{\rm BB}$ are numerical coefficients given in Appendix B. At large x both functions, $f_{\rm AB}(x)$ and $f_{\rm BB}(x)$, should represent outgoing waves:

$$\begin{bmatrix} f_{\rm AB}(x) \\ f_{\rm BB}(x) \end{bmatrix} \underset{x\to\infty}{\propto} \frac{\exp(ikx)}{x^{3/2}}. \quad (53)$$

We mention that at the unitary limit, the solution is known analytically and f_{ij} are expressed in terms of the outgoing Hankel function

$$\begin{bmatrix} f_{\rm AB}(x) \\ f_{\rm BB}(x) \end{bmatrix} = \begin{pmatrix} C_{\rm AB} \\ C_{\rm BB} \end{pmatrix} \frac{\sinh(s_0\pi)}{e^{s_0\pi}}\, 2^{is_0}\Gamma(1+is_0)\frac{H^{(1)}_{is_0}(kx)}{x}, \quad (54)$$

which, matched with Eq. (52), gives the limiting expression, Eq. (10).

In order to calculate s_{11} for arbitrary $(ka_{\rm AB}, ka_{\rm BB})$ we switch to momentum representations, where the STM equations are written

$$\begin{aligned} (\sqrt{p^2-k^2-i0^+} - 1/a_{\rm AB})f_{\rm AB} - \hat{L}_{k^2,\phi} f_{\rm AB} - \hat{L}_{k^2,\theta} f_{\rm BB} &= 0, \\ (\sqrt{p^2-k^2-i0^+} - 2\sin\theta/a_{\rm BB})f_{\rm BB} - 2\hat{L}_{k^2,\theta} f_{\rm AB} &= 0, \end{aligned} \quad (55)$$

where $f_{ij}(p) = \int f_{ij}(x)\exp(-i\mathbf{px})d^3x$,

$$\begin{aligned} &\hat{L}_{k^2,\alpha} f(p) \\ &= \frac{1}{\pi\sin 2\alpha}\int_0^\infty dp'\, f(p')\frac{p'}{p} \\ &\quad \times \ln\left(\frac{p'^2 + 2pp'\sin\alpha + p^2 - k^2\cos^2\alpha - i0^+}{p'^2 - 2pp'\sin\alpha + p^2 - k^2\cos^2\alpha - i0^+}\right), \end{aligned} \quad (56)$$

ϕ and θ are the mass angles defined in Eqs. (2) and (3), and the inclusion of a small positive 0^+ indicates that k is slightly shifted into the upper complex half-plane, thus fixing the branch cuts of the logarithm and square root and ensuring the presence of only the outgoing wave, (53), in the solution. The boundary condition, (52), now reads

$$\begin{bmatrix} f_{\rm AB}(p) \\ f_{\rm BB}(p) \end{bmatrix} \underset{p\to\infty}{\simeq} \begin{pmatrix} C_{\rm AB} \\ C_{\rm BB} \end{pmatrix} \frac{2\pi^2 s_0}{\sinh(\pi s_0/2)} \left[\frac{1}{\Gamma(1-is_0)}\frac{(p/k)^{-is_0}}{p^2} + s_{11}\frac{1}{\Gamma(1+is_0)}\frac{(p/k)^{is_0}}{p^2}\right]. \quad (57)$$

We then perform a complex scaling transformation. We use the fact that s_{11} depends only on the products $a_{\rm AB}k$ and $a_{\rm BB}k$ and replace $k \to i$, $a_{ij} \to -ia_{ij}k$ in Eq. (55). Equivalently, this can be done by rotating the integration contour over p' in Eq. (56) to the negative imaginary axis. The obtained STM

equations,

$$(\sqrt{p^2+1} - i/a_{\rm AB}k) f_{\rm AB} - \hat{L}_{-1,\phi} f_{\rm AB} - \hat{L}_{-1,\theta} f_{\rm BB} = 0,$$
$$(\sqrt{p^2+1} - 2i\sin\theta/a_{\rm BB}k) f_{\rm BB} - 2\hat{L}_{-1,\theta} f_{\rm AB} = 0, \tag{58}$$

do not contain singularities in the kernels and can be efficiently solved numerically. We deduce s_{11} from matching the solution with the asymptotic form

$$\begin{bmatrix} f_{\rm AB}(p) \\ f_{\rm BB}(p) \end{bmatrix} \underset{p\to\infty}{\propto} \begin{pmatrix} C_{\rm AB} \\ C_{\rm BB} \end{pmatrix} \left[p^{-2-is_0} + s_{11} e^{\pi s_0} \times \frac{\Gamma(1-is_0)}{\Gamma(1+is_0)} p^{-2+is_0} \right] \tag{59}$$

for any given set $a_{\rm AB}k$ and $a_{\rm BB}k$. More precisely, we use the following procedure. We introduce new unknown functions $g_{\rm AB}(p)$ and $g_{\rm BB}(p)$ such that $f_{ij}(p) \propto [p^{-2-is_0} + g_{ij}(p)]$ [the proportionality coefficients follow from Eq. (57) but are irrelevant for the determination of s_{11}] and require that for large momenta $g_{ij}(p) \propto p^{-2+is_0}$. Equations (58) become a set of linear inhomogeneous equations for g_{AB} and g_{BB}, which we solve by discretizing p and inverting the corresponding discrete analog of the operator on the left-hand side of Eqs. (58). The final result is given by $s_{11} = e^{-\pi s_0}\Gamma(1+is_0)/\Gamma(1-is_0)\lim_{p\to\infty} g_{ij}(p)p^{2-is_0}$ independent of the choice $g_{\rm AB}$ or $g_{\rm BB}$.

Case i is obtained by setting $f_{\rm BB} = C_{\rm BB} = a_{\rm BB} = 0$ in the above analysis and omitting the second lines in the STM equations, (55) and (58). Various properties of the ABB system in case i have been studied by using the STM equation derived in this case from the effective field theory [34]. The STM equations in both case i and case ii have been employed in a recent study of the single-particle momentum distribution of heteronuclear Efimov trimers [37].

Another point which is useful to mention is that Braaten *et al.* [28] have developed a slightly different method for calculating s_{11} in the case of three identical bosons. They also use the STM equation but deduce s_{11} from solving the atom-dimer scattering problem for positive a above the dimer breakup threshold. We note that their approach works well for small $ka > 0$, whereas ours is optimal for large ka, either positive or negative. In fact, $s_{11}(-a_{\rm AB}k, -a_{\rm BB}k) = e^{-2\pi s_0}/s_{11}^*(a_{\rm AB}k, a_{\rm BB}k)$. This relation follows from Eq. (59) and the observation that if f_{ij} is the solution of Eqs. (58) for a_{ij}, then f_{ij}^* is the solution for $a_{ij} = -a_{ij}$.

V. SUMMARY AND OUTLOOK

In this paper we have obtained the finite-temperature three-body loss rate constant within the zero-range theory for the ABB system, with $a_{\rm AB} < 0$, and no BB interaction (case i) or $a_{\rm BB} < 0$ (case ii). For a given mass ratio, we expressed the rate constant in terms of temperature T, three-body parameter R_0, inelasticity parameter η, and a universal function s_{11} that depends on $ka_{\rm AB}$, as well as on $ka_{\rm BB}$ in case ii, where k is the three-body collision momentum. We developed a numerical method based on complex scaling for computing the function s_{11} and perform this calculation for two experimentally relevant cases: ^{6}Li-^{133}Cs-^{133}Cs and ^{6}Li-^{87}Rb-^{87}Rb. The knowledge of s_{11} reduces the problem of computing the loss rate to a simple thermal averaging integral over k for any desired T, R_0, and η. We expect that these results, combined with experimental data, will be useful for precise tests of universality and determinations of R_0 and η. For ^{6}Li-^{133}Cs-^{133}Cs we find that inclusion of the CsCs interaction leads to a significant enhancement of the loss rate constant. This is in spite of the fact that the scaling factors in cases i and ii are very close for this high mass ratio. The enhanced loss rate is likely to be explained by an enhanced probability of finding two Cs atoms close to each other in the CsCs-interacting case.

In deriving the loss rate coefficient we explicitly constructed the hyperangular wave function $\Phi_3(\mathbf{\Omega})$ corresponding to the long-distance three-atom channel which is connected by a unitary 2×2 matrix with the Efimovian wave at small hyper-radii. The corresponding S-matrix formalism smoothly connects with the exactly solvable unitarity limit. The three-body loss problem reduces to a simple Fabry-Perot interferometer with two partially reflecting mirrors.

Three-body systems at zero total energy are known to be analytically solvable in the zero-range approximation if there is only one relevant scattering length (three identical bosons [40,48–51], ABB system in case i [34], ABB system with fermionic B particles [46]). A theoretical challenge that we can formulate now is to generalize these approaches to the ABB system in case ii at vanishing total energy. In particular, it would be interesting to obtain an analytic expression for the loss rate constant at zero temperature (dash-dotted line in Fig. 2).

Note added. Recently, we became aware of a related work [52] that uses the adiabatic hyperspherical approximation and also finds a strong effect of the BB interaction.

ACKNOWLEDGMENTS

We thank A. Bulgac, F. Chevy, A. Grier, R. Grimm, and E. Kuhnle for fruitful discussions and acknowledge support from the IFRAF Institute and the Institute for Nuclear Theory under the program Universality in Few-Body Systems: Theoretical Challenges and New Directions, INT-14-1. The research leading to these results received funding from the European Research Council under the European Community's Seventh Framework Program (FR7/2007-2013; Grant Agreement No. 341197), ERC (Grant Thermodynamix), and IFRAF-NanoK (Grant Atomix).

APPENDIX A: BASIC PROPERTIES OF THE s MATRIX

Here we derive some basic properties of the s matrix that are stated and used in the main text. Let us first give a proper definition of the s matrix. In addition to the state Ψ_1 defined above, let us define the state Ψ_m for $m \geqslant 3$ as the solution of the Schrödinger equation with the two-body contact condition, Eqs. (16) and (17), whose asymptotic behavior contains an incoming wave of unit amplitude in channel m and a purely outgoing wave in the other channels; the coefficients of the outgoing waves then define the column $(s_{nm})_{n\in\mathcal{C}}$ of the s matrix:

$$\begin{cases} \Psi_m \underset{R\to 0}{\simeq} s_{1m}\,\psi_1^{\rm out} \\ \Psi_m \underset{R\to\infty}{\simeq} \psi_m^{\rm in} + \sum_{n\geqslant 3} s_{nm}\,\psi_n^{\rm out}. \end{cases} \tag{A1}$$

A useful lemma is that for an arbitrary state Ψ solving Schrödinger's equation with the two-body contact condition, Eqs. (16) and (17), the in- and out-amplitudes [defined in Eqs. (45) and (46)] are constrained by

$$\sum_{n\in\mathcal{C}} \left|A_n^{\rm in}\right|^2 = \sum_{n\in\mathcal{C}} \left|A_n^{\rm out}\right|^2. \tag{A2}$$

This follows from the conservation of probability. More precisely, the flux through a hypersurface $\mathcal{S}$ [defined as in Eqs. (19) and (20)] is independent of $\mathcal{S}$. Taking for $\mathcal{S}$ a hypersphere of very small or very large radius, the flux, respectively, equals $|A_1^{\rm out}|^2 - |A_1^{\rm in}|^2$ or $\sum_{n\geqslant 3}(|A_n^{\rm out}|^2 - |A_n^{\rm in}|^2)$.

A useful consequence is that if Ψ and Ψ' are two solutions of Eqs. (16) and (17) with the same in-amplitudes, then their out-amplitudes are also equal. This follows from applying the above lemma to $\Psi - \Psi'$. The linear relation between out- and in-amplitudes, Eq. (47), then follows by noting that Ψ and $\sum_{n\in\mathcal{C}} A_n^{\rm in}\,\Psi_n$ have equal in-amplitudes and hence equal out-amplitudes.

Let us now check that the matrix s_{nm} is unitary. Physically this comes again from the conservation of probability. More precisely, applying the lemma, Eq. (A2), to the state $\Psi = \Psi_n + \alpha\,\Psi_{n'}$, where $n \neq n'$ and α is an arbitrary complex number, we get

$$1 + |\alpha|^2 = \sum_{m\in\mathcal{C}} |s_{mn} + \alpha\, s_{mn'}|^2. \tag{A3}$$

Taking $\alpha = 0$ yields

$$\sum_m |s_{mn}|^2 = 1. \tag{A4}$$

Thus (A3) simplifies to $\mathrm{Re}(\alpha \sum_m s_{mn}^* s_{mn'}) = 0$ for any α, which implies

$$\sum_m s_{mn}^* s_{mn'} = 0. \tag{A5}$$

Let us now check that s_{nm} is symmetric. Physically, this follows from time-reversal invariance. More precisely, we consider the state Ψ_n^*, and note that it has the same in-amplitudes as $\sum_{m\in\mathcal{C}} s_{mn}^*\,\Psi_m$ and, hence, also the same out-ampltiudes. This yields $s\cdot s^* = \mathbf{1}$, and hence, since s is unitary, $s = s^T$.

APPENDIX B: DETERMINATION OF s_0, $C_{\rm AB}$, AND $C_{\rm BB}$

The STM equations can be used to calculate s_0 and the ratio of $C_{\rm AB}$ and $C_{\rm BB}$. To this end, it suffices to consider the scale-invariant case where the interaction is at the unitary limit and the energy is 0.

Let us first consider case ii. A solution of the STM equations, (55), for $k = 0$, is given by the ansatz [37]

$$\begin{bmatrix} f_{\rm AB}(x) \\ f_{\rm BB}(x) \end{bmatrix} = \begin{pmatrix} C_{\rm AB} \\ C_{\rm BB} \end{pmatrix} \frac{p^{is_0}}{p^2}.$$

Indeed, we have $\hat{L}_{0,\alpha}\, p^{is_0}/p^2 = \lambda(s_0,\alpha)\, p^{is_0}/p$, where the function λ is defined by Eq. (8). The STM equations then become a 2×2 homogeneous system of linear algebraic equations for $C_{\rm AB}$ and $C_{\rm BB}$:

$$\begin{pmatrix} 1-\lambda(s_0,\phi) & -\lambda(s_0,\theta) \\ -2\lambda(s_0,\theta) & 1 \end{pmatrix} \begin{pmatrix} C_{\rm AB} \\ C_{\rm BB} \end{pmatrix} = 0. \tag{B1}$$

The requirement that the determinant of the 2×2 matrix in Eq. (B1) vanish gives the implicit equation for s_0, Eq. (7). The ratio between $C_{\rm AB}$ and $C_{\rm BB}$ is then fixed by $C_{\rm BB} = 2\lambda(s_0,\theta) C_{\rm AB}$ and we can choose these coefficients to be real.

In case i, one should formally set $C_{\rm BB} = 0$ in the above analysis.

Finally, we note that, even though all that is used for the computation of s_{11} in Sec. IV is the ratio of $C_{\rm AB}$ and $C_{\rm BB}$, their absolute values can also be determined, thanks to the expression of the normalized wave function $\phi_{is_0}(\mathbf{\Omega})$ given in Appendix C. Indeed, Eqs. (41), (50), (C3), and (C4) yield straightforwardly

$$\begin{pmatrix} C_{\rm AB} \\ C_{\rm BB} \end{pmatrix} = 4\pi \sinh\left(s_0 \frac{\pi}{2}\right) \sqrt{\frac{m}{2s_0}} \begin{pmatrix} \mathcal{C}_{\rm AB} \\ \mathcal{C}_{\rm BB} \end{pmatrix}, \tag{B2}$$

the absolute values of $\mathcal{C}_{\rm AB}$ and $\mathcal{C}_{\rm BB}$ being determined by Eq. (C7).

APPENDIX C: NORMALIZED WAVE-FUNCTION AND CONTACT PARAMETERS OF A HETERONUCLEAR EFIMOV TRIMER

In this Appendix, we consider three-body bound states, i.e., negative-energy solutions of the zero-range model [defined by the three-body Schrödinger equation, Eq. (16), the two-body contact condition, Eq. (17), and the three-body contact condition, Eq. (18)], at the unitary limit, Eq. (4), and without losses ($\eta = 0$). We provide the analytical expressions of their normalized wave functions and their contact parameters. We consider case ii throughout this Appendix. The content of this Appendix also applies to case i provided $\mathcal{C}_{\rm BB}$ is formally set to 0.

1. Wave function

The trimer's wave function is written [24]

$$\psi(\mathbf{R}) = \frac{F(R)}{R^2}\,\phi_{is_0}(\mathbf{\Omega}), \tag{C1}$$

where the hyper-radial part is proportional to a Bessel function

$$F(R) = \mathcal{N}\, K_{is_0}(\sqrt{m|E|}\,R), \tag{C2}$$

and the hyperangular part is written

$$\phi_{is_0}(\mathbf{\Omega}) = (1+P)\,\mathcal{C}_{\rm AB}\frac{\varphi(\alpha)}{\sin\alpha\cos\alpha} + \mathcal{C}_{\rm BB}\frac{\varphi(\beta)}{\sin\beta\cos\beta}, \tag{C3}$$

where

$$\varphi(\alpha) = \sinh\left[s_0\left(\frac{\pi}{2} - \alpha\right)\right], \tag{C4}$$

α and β being hyperangles defined by

$$x = R\,\cos\alpha, \quad y = R\,\sin\alpha$$

and

$$X = R\,\cos\beta, \quad Y = R\,\sin\beta,$$

the Jacobi coordinates (x,y) and (X,Y) being defined in Eqs. (11) and (51).

Imposing the two-body contact conditions, Eqs. (17), yields that $\mathcal{C}_{\rm AB}$ and $\mathcal{C}_{\rm BB}$ satisfy the same matrix equation, Eq. (B1), as $C_{\rm AB}$ and $C_{\rm BB}$, which again yields Eq. (7) for s_0, as well as

$$\mathcal{C}_{\rm BB} = 2\lambda(s_0,\theta)\mathcal{C}_{\rm AB}. \tag{C5}$$

The spectrum is

$$E_n = -\frac{1}{m R_0^2}\, 4\, e^{2\arg\Gamma(1+is_0)/s_0}\, e^{-n\,2\pi/s_0}, \quad n \in \mathbb{Z}, \tag{C6}$$

as obtained by imposing the three-body contact condition, Eq. (18).

The normalization of the wave function can be done analytically, generalizing [53] to the heteronuclear case. For the hyperangular part, we take $(\phi_{is_0}|\phi_{is_0}) = 1$ for the hyperangular scalar product introduced in Eq. (27). This leads to

$$\left(2\mathcal{C}_{\rm AB}^{\,2} + \mathcal{C}_{\rm BB}^{\,2}\right) Q(\pi/2) + 2\mathcal{C}_{\rm AB}^{\,2}\, Q(\phi) + 4\mathcal{C}_{\rm AB}\mathcal{C}_{\rm BB}\, Q(\theta) = 1, \tag{C7}$$

where

$$Q(\alpha) = \frac{8\pi^2}{s_0 \sin 2\alpha}\left[\pi \cosh\left(s_0\frac{\pi}{2}\right)\sinh(s_0\,\alpha) - 2\alpha \sinh\left(s_0\frac{\pi}{2}\right)\cosh(s_0\,\alpha)\right] \tag{C8}$$

and

$$Q(\pi/2) \equiv \lim_{\alpha\to\pi/2} Q(\alpha) = 4\pi^2[\sinh(s_0\pi)/s_0 - \pi].$$

In order to normalize the hyper-radial wave function, it is convenient to consider that the three particles are subject to an external harmonic trapping potential of vanishing frequency [53], so that one can impose $\int d^3r_1 d^3r_2 d^3r_3 |\Psi(\mathbf{r}_1,\mathbf{r}_2,\mathbf{r}_3)|^2 = 1$, where Ψ equals $\psi(\mathbf{R})$ times a center-of-mass wave function, $\psi_{\rm CM}(\mathbf{C})$, normalized to $\int d^3C |\psi_{\rm CM}(\mathbf{C})|^2 = 1$. Due to the Jacobian, Eq. (23), this gives $\int_0^\infty dR\, R\, |F(R)|^2 = \cos^{-3}\phi$. The integral over R has a known expression [54], which finally yields

$$\mathcal{N} = \sqrt{\frac{2m|E|\,\sinh(s_0\pi)}{s_0\pi\,\cos^3\phi}}. \tag{C9}$$

2. Contact parameters

From this normalized wave function, it is straightforward to deduce the contact parameters of an Efimov trimer, i.e., the partial derivatives of its energy with respect to the scattering lengths taken at a fixed three-body parameter. Indeed, as shown in Ref. [55], $(\partial E/\partial a_{ij})_{R_0}$ is proportional to the norm of the function A_{ij} appearing in the two-body contact condition, Eq. (17). This yields

$$\left.\frac{\partial E}{\partial(-1/a_{\rm AB})}\right|_{R_0} = \mathcal{C}_{\rm AB}^{\,2}\sqrt{\frac{|E|}{m}}\, 16\pi^3\, \frac{\tanh(s_0\pi)\,\sinh^2(s_0\pi/2)}{s_0}, \tag{C10}$$

$$\left.\frac{\partial E}{\partial(-1/a_{\rm BB})}\right|_{R_0} = \mathcal{C}_{\rm BB}^{\,2}\sqrt{\frac{|E|}{m}}\, 16\pi^3\, \frac{\tanh(s_0\pi)\,\sinh^2(s_0\pi/2)}{s_0} \times \sin\theta. \tag{C11}$$

This generalizes to the heteronuclear case the result obtained in [53] for three identical bosons.

APPENDIX D: EXPANSION OF s_{11} AROUND THE UNITARY LIMIT

This Appendix concerns leading-order corrections to s_{11} near the unitary limit. We start by stating the results. In case ii, when $k|a_{\rm AB}|$ and $k|a_{\rm BB}|$ tend to ∞, we have the expansion

$$s_{11} \approx s_{11}^\infty\left[1 - 16\,\pi^3\,\tanh(s_0\pi)\,\sinh^2\left(s_0\frac{\pi}{2}\right) \times\left(\frac{\mathcal{C}_{\rm AB}^{\,2}}{a_{\rm AB}k} + \frac{\mathcal{C}_{\rm BB}^{\,2}\,\sin\theta}{a_{\rm BB}k}\right)\right], \tag{D1}$$

where s_{11}^∞ is given by Eq. (10) and the coefficients $\mathcal{C}_{\rm AB}$ and $\mathcal{C}_{\rm BB}$ are derived from Eqs. (C5) and (C7). In case i, the expansion for $k|a_{\rm AB}| \to \infty$ is given by formally setting $\mathcal{C}_{\rm BB} = 0$ in Eqs. (D1) and (C7).

We present the derivation in case ii (case i is treated similarly with obvious simplifications). We employ the same complex scaling procedure as in Sec. IV, now at the level of the Schrödinger equation. Namely, we assume that the function $Z \mapsto \Psi_1(Z\,\mathbf{R})$, defined *a priori* for real positive Z, can be analytically continued to the quadrant $0 \leqslant \mathrm{Arg}\, Z \leqslant \pi/2$, and we consider the scaled wave function $\tilde\Psi_1(\tilde{\mathbf{R}}) \equiv \Psi_1(i\,\tilde{\mathbf{R}}/k)$, where $\tilde{\mathbf{R}}$ has real coordinates. The Schrödinger equation $-\Delta_{\mathbf{R}}\Psi_1 = k^2\,\Psi_1$ then becomes $-\Delta_{\tilde{\mathbf{R}}}\tilde\Psi_1 = -\tilde\Psi_1$. Furthermore, the large-distance behavior $\Psi_1 \propto e^{ikR}$ gives $\tilde\Psi_1 \propto e^{-\tilde R}$ after analytic continuation. Finally, because Ψ_1 satisfies the two-body contact conditions with scattering lengths $(a_{\rm AB},a_{\rm BB})$, $\tilde\Psi_1$ satisfies the two-body contact conditions with the scaled scattering lengths

$$(\tilde a_{\rm AB},\tilde a_{\rm BB}) = (a_{\rm AB},a_{\rm BB})\,k/i. \tag{D2}$$

The short-distance behavior $\Psi_1 \propto (kR)^{is_0} + s_{11}\,(kR)^{-is_0}$ turns into $\tilde\Psi_1 \propto \tilde R^{is_0} + s_{11}\,e^{\pi s_0}\,\tilde R^{-is_0}$, which we rewrite as $\tilde\Psi_1 \propto (\tilde R/\tilde R_0)^{-is_0} - (\tilde R/\tilde R_0)^{is_0}$, where $\tilde R_0$ can be viewed as an effective (in general, complex) three-body parameter, related to s_{11} by $s_{11}\,e^{\pi s_0} = -\tilde R_0^{\,2is_0}$. Summarizing, the scaled wave function corresponds to a bound trimer state, of fixed energy $-1/m$, with imaginary scattering lengths and a complex three-body parameter.

At the unitary limit, the rescaling of the scattering lengths, Eq. (D2), has no effect, and $\tilde\Psi_1$ is the wave function of a standard Efimov trimer. Hence its effective three-body parameter $\tilde R_0$ is real and is related to its energy, $-1/m$, as in Eq. (C6). This allows us to retrieve the expression, Eq. (10), of s_{11}^∞.

If we move slightly away from the unitary limit by turning on small finite inverse scattering lengths, $\tilde R_0$ has to shift in such a way that the scaled energy remains fixed. But the partial derivatives of the energy with respect to the inverse scattering lengths are given by the contact parameters, computed in Appendix C. The partial derivative of the energy with respect to the three-body parameter, on the other hand, is obtained easily from the simple relation between the energy and the three-body parameter valid at the scale-invariant point. This yields the desired result, Eq. (D1).

APPENDIX E: THREE IDENTICAL BOSONS

The case of recombination among three bosons in the same internal state, which is the subject of Ref. [10], can be recovered from the present article, *modulo* minor modifications given in this Appendix. One sets $m_A = m_B = m$ so that $\phi = \theta = \pi/6$, and $a_{AB} = a_{BB} =: a$ (case i does not exist any more). In Eq. (6) the right-hand side is multiplied by 2. For the symmetrization and normalization of the plane wave, in Eq. (14), the term $(1 + P)/\sqrt{2}$ is replaced by $(\sum_\sigma P_\sigma)/\sqrt{3!}$, where the sum over σ now runs over the 3! permutations of the three particles. As a consequence, the right-hand side of Eq. (39) (and of its finite-a generalization) gets multiplied by $\sqrt{3}$. Furthermore, in Eq. (22) the right-hand side contains an additional factor $1/3$. The additional factors cancel out in the final result for K and Eq. (9) is unchanged.

As far as the calculation of the function s_{11} is concerned, Sec. IV remains entirely valid in case BBB but gets simplified by observing that $f_{AB} = f_{BB}$ and $C_{AB} = C_{BB}$, which leads to the usual single STM equation. Similarly, all analytic results in Appendixes C and D reproduce the known BBB ones (in this case $\mathcal{C}_{AB} = \mathcal{C}_{BB}$, and $\partial_{1/a_{AB}} + \partial_{1/a_{BB}}$ should be replaced by $\partial_{1/a}$). For completeness we also mention the relation between a_- and R_0 in this case, $a_- \approx -1.017 R_0$.

[1] E. Braaten and H.-W. Hammer, Ann. Phys. **322**, 120 (2007).
[2] F. Ferlaino, A. Zenesini, M. Berninger, B. Huang, H.-C. Nägerl, and R. Grimm, Few-Body Syst. **51**, 113 (2011).
[3] N. Gross, Z. Shotan, O. Machtey, S. Kokkelmans, and L. Khaykovich, C. R. Physique **12**, 4 (2011).
[4] T. Kraemer, M. Mark, P. Waldburger, J. G. Danzl, C. Chin, B. Engeser, A. D. Lange, K. Pilch, A. Jaakkola, H.-C. Naegerl, and R. Grimm, Nature **440**, 315 (2006).
[5] N. Gross, Z. Shotan, S. Kokkelmans, and L. Khaykovich, Phys. Rev. Lett. **103**, 163202 (2009).
[6] N. Gross, Z. Shotan, S. Kokkelmans, and L. Khaykovich, Phys. Rev. Lett. **105**, 103203 (2010).
[7] M. Berninger, A. Zenesini, B. Huang, W. Harm, H.-C. Nägerl, F. Ferlaino, R. Grimm, P. S. Julienne, and J. M. Hutson, Phys. Rev. Lett. **107**, 120401 (2011).
[8] R. J. Wild, P. Makotyn, J. M. Pino, E. A. Cornell, and D. S. Jin, Phys. Rev. Lett. **108**, 145305 (2012).
[9] S. Roy, M. Landini, A. Trenkwalder, G. Semeghini, G. Spagnolli, A. Simoni, M. Fattori, M. Inguscio, and G. Modugno, Phys. Rev. Lett. **111**, 053202 (2013).
[10] B. S. Rem, A. T. Grier, I. Ferrier-Barbut, U. Eismann, T. Langen, N. Navon, L. Khaykovich, F. Werner, D. S. Petrov, F. Chevy, and C. Salomon, Phys. Rev. Lett. **110**, 163202 (2013).
[11] R. J. Fletcher, A. L. Gaunt, N. Navon, R. P. Smith, and Z. Hadzibabic, Phys. Rev. Lett. **111**, 125303 (2013).
[12] B. Huang, L. A. Sidorenkov, R. Grimm, and J. M. Hutson, Phys. Rev. Lett. **112**, 190401 (2014).
[13] B. Huang, L. A. Sidorenkov, and R. Grimm, Phys. Rev. A **91**, 063622 (2015).
[14] U. Eismann, L. Khaykovich, S. Laurent, I. Ferrier-Barbut, B. S. Rem, A. T. Grier, M. Delehaye, F. Chevy, C. Salomon, L.-C. Ha, and C. Chin, arXiv:1505.04523.
[15] T. B. Ottenstein, T. Lompe, M. Kohnen, A. N. Wenz, and S. Jochim, Phys. Rev. Lett. **101**, 203202 (2008).
[16] J. R. Williams, E. L. Hazlett, J. H. Huckans, R. W. Stites, Y. Zhang, and K. M. O'Hara, Phys. Rev. Lett. **103**, 130404 (2009).
[17] B. Huang, K. M. O'Hara, R. Grimm, J. M. Hutson, and D. S. Petrov, Phys. Rev. A **90**, 043636 (2014).
[18] G. Barontini, C. Weber, F. Rabatti, J. Catani, G. Thalhammer, M. Inguscio, and F. Minardi, Phys. Rev. Lett. **103**, 043201 (2009).
[19] R. S. Bloom, M.-G. Hu, T. D. Cumby, and D. S. Jin, Phys. Rev. Lett. **111**, 105301 (2013).
[20] R. Pires, J. Ulmanis, S. Häfner, M. Repp, A. Arias, E. D. Kuhnle, and M. Weidemüller, Phys. Rev. Lett. **112**, 250404 (2014).
[21] S.-K. Tung, K. Jiménez-García, J. Johansen, C. V. Parker, and C. Chin, Phys. Rev. Lett. **113**, 240402 (2014).
[22] J. P. D'Incao, H. Suno, and B. D. Esry, Phys. Rev. Lett. **93**, 123201 (2004).
[23] V. N. Efimov, Yad. Fiz. **12**, 1080 (1970) [Sov. J. Nucl. Phys. **12**, 589 (1971)].
[24] V. Efimov, Nucl. Phys. A **210**, 157 (1973).
[25] J. P. D'Incao and B. D. Esry, Phys. Rev. A **73**, 030703(R) (2006).
[26] V. Efimov, Yad. Fiz. **29**, 1058 (1979) [Sov. J. Nucl. Phys. **29**, 546 (1979)].
[27] E. Braaten and H.-W. Hammer, Phys. Rep. **428**, 259 (2006).
[28] E. Braaten, H.-W. Hammer, D. Kang, and L. Platter, Phys. Rev. A **78**, 043605 (2008).
[29] A. Marte, T. Volz, J. Schuster, S. Dürr, G. Rempe, E. G. M. van Kempen, and B. J. Verhaar, Phys. Rev. Lett. **89**, 283202 (2002).
[30] C. Chin, R. Grimm, P. Julienne, and E. Tiesinga, Rev. Mod. Phys. **82**, 1225 (2010).
[31] B. Deh, C. Marzok, C. Zimmermann, and P. W. Courteille, Phys. Rev. A **77**, 010701 (2008).
[32] C. Marzok, B. Deh, C. Zimmermann, P. W. Courteille, E. Tiemann, Y. V. Vanne, and A. Saenz, Phys. Rev. A **79**, 012717 (2009).
[33] D. S. Petrov, C. Salomon, and G. V. Shlyapnikov, J. Phys. B **38**, S645 (2005).
[34] K. Helfrich, H.-W. Hammer, and D. S. Petrov, Phys. Rev. A **81**, 042715 (2010).
[35] M. Berninger, A. Zenesini, B. Huang, W. Harm, H.-C. Nägerl, F. Ferlaino, R. Grimm, P. S. Julienne, and J. M. Hutson, Phys. Rev. A **87**, 032517 (2013).
[36] A. C. Fonseca, E. F. Redish, and P. E. Shanley, Nucl. Phys. A **320**, 273 (1979).
[37] M. T. Yamashita, F. F. Bellotti, T. Frederico, D. V. Fedorov, A. S. Jensen, and N. T. Zinner, Phys. Rev. A **87**, 062702 (2013).
[38] J. Ulmanis, S. Häfner, R. Pires, E. D. Kuhnle, M. Weidemüller, and E. Tiemann, New J. Phys. **17**, 055009 (2015).
[39] A. Derevianko, J. F. Babb, and A. Dalgarno, Phys. Rev. A **63**, 052704 (2001).
[40] D. S. Petrov, in *Proceedings of the Les Houches Summer Schools, Session 94*, edited by C. Salomon, G. V. Shlyapnikov, and L. F. Cugliandolo (Oxford University Press, Oxford, UK, 2013).

[41] S.-K. Tung, C. Parker, J. Johansen, C. Chin, Y. Wang, and P. S. Julienne, Phys. Rev. A **87**, 010702 (2013).
[42] Y. Castin and F. Werner, in *The BCS-BEC Crossover and the Unitary Fermi Gas*, edited by W. Zwerger, Lecture Notes in Physics Vol. 836 (Springer, Heidelberg, 2012), p. 127 .
[43] Y. Wang, J. Wang, J. P. D'Incao, and C. H. Greene, Phys. Rev. Lett. **109**, 243201 (2012).
[44] Y. Wang and B. D. Esry, New J. Phys. **13**, 035025 (2011).
[45] S. Laurent, X. Leyronas, and F. Chevy, Phys. Rev. Lett. **113**, 220601 (2014).
[46] D. S. Petrov, Phys. Rev. A **67**, 010703 (2003).
[47] Y. Castin and E. Tignone, Phys. Rev. A **84**, 062704 (2011).
[48] J. H. Macek, S. Ovchinnikov, and G. Gasaneo, Phys. Rev. A **72**, 032709 (2005).
[49] J. H. Macek, S. Y. Ovchinnikov, and G. Gasaneo, Phys. Rev. A **73**, 032704 (2006).
[50] A. O. Gogolin, C. Mora, and R. Egger, Phys. Rev. Lett. **100**, 140404 (2008).
[51] C. Mora, A. O. Gogolin, and R. Egger, C. R. Physique **12**, 27 (2011).
[52] M. Mikkelsen, A. S. Jensen, D. V. Fedorov, and N. T. Zinner, J. Phys. B **48**, 085301 (2015).
[53] Y. Castin and F. Werner, Phys. Rev. A **83**, 063614 (2011).
[54] I. S. Gradshteyn and I. M. Ryzhik, *Tables of Integrals, Series, and Products*, 5th ed., edited by A. Jeffrey (Academic Press, New York, 1994).
[55] F. Werner and Y. Castin, Phys. Rev. A **86**, 053633 (2012).